Research Article *Open Access*

Journal of Scientific Engineering Advances

ISSN: 3071-0723

Assessment of Walking Ability in Parkinson's Patients Using Three-Dimensional Plantar Pressure Sensors

Terry Zhang

Kent School, USA

Citation: *Terry Zhang (2026) Assessment of Walking Ability in Parkinson's Patients Using Three-Dimensional Plantar Pressure sensors. J. of Sci Eng Advances 2(5) 1-9. WMJ/JSEA-162*

Abstract

As the world population enters an aging era, the situation of Parkinson's disease is becoming increasingly severe. The clinical manifestations of Parkinson's patients mainly include tremors, walking disorders, muscle rigidity, and bradykinesia, among which walking disorders and bradykinesia are the more obvious features of Parkinson's patients. The existing gait analysis methods mainly include image analysis, wearable sensor analysis, and plantar pressure testing platform analysis. Among them, wearable sensor analysis is expected to solve the long-term and low-cost gait detection needs. However, currently wearable sensors cannot measure the tangential force on the sole of the foot, resulting in the inability to obtain complete plantar force information of patients, which poses difficulties for more accurate gait analysis. This project designs a three-dimensional force sensor and measurement method for the sole of the foot, and uses machine learning algorithms to evaluate the walking ability of Parkinson's patients.

***Corresponding author**: Terry Zhang, Kent School, USA.

Submitted: 15.09.2026 **Accepted**: 21.09.2026 **Published**: 17.10.2026

Keywords: Parkinson's Disease, 3D Force, Plantar Pressure

Introduction

Parkinson's disease (PD) is a common neurodegenerative disease that mainly affects middle-aged and elderly people, but there has also been an increase in young cases in recent years [1]. The core pathological feature is the degeneration and death of dopaminergic neurons in the substantia nigra of the midbrain, leading to a significant decrease in dopamine content in the striatum and causing motor regulation disorders. According to authoritative medical reports, the number of Parkinson's patients worldwide is expected to approach 10 million by 2025 [2].

Nowadays, the diagnosis of Parkinson's disease remains

a huge challenge. Clinics and hospitals lack constant check-ups on patients' status. The analysis method based on plantar pressure and gait data is believed to achieve effective diagnosis of Parkinson's disease [3]. The measurement of plantar pressure mainly relies on platform-based sensors or in-shoe sensors [4]. An in-shoe-based planar sensor is a wearable measurement system that has the advantages of long-term use and low cost [5]. But, currently, foot pressure sensors can only measure positive pressure. Unable to obtain a true 3D pressure distribution on the sole of the foot. This limits its accuracy in diagnosing Parkinson's disease. On the other hand, the big data of plantar pressure needs to rely on AI models for analysis and processing, and complete diagnosis.

In this work, we presented a 3D planar measurement system based on a piezoresistive sensor. Using this system to collect three-dimensional pressure distribution data of patients' soles. A CRNN neural network was used to analyze the data and determine whether the patient has Parkinson's disease. This sensor can be used for early diagnosis and treatment efficacy evaluation of Parkinson's disease.

Design and Fabrication

Principle

In this work, we developed a 3D plantar force measurement for estimating the status of Parkinson's patient. The system operates by transducing the three-dimensional plantar force vector into measurable electrical signals via custom anisotropic silicone pyramids interfaced with four single-axis piezoresistive sensors. Each pyramid's geometry mechanically converts an

applied 3D force into a distinct pattern of differential compression across its base. A vertical force compresses all four underlying sensors nearly equally, while shear forces along the x- or y-axes create asymmetric strain, with opposing sensor pairs experiencing higher compression. This differential mechanical response is the foundation for directional force discrimination.

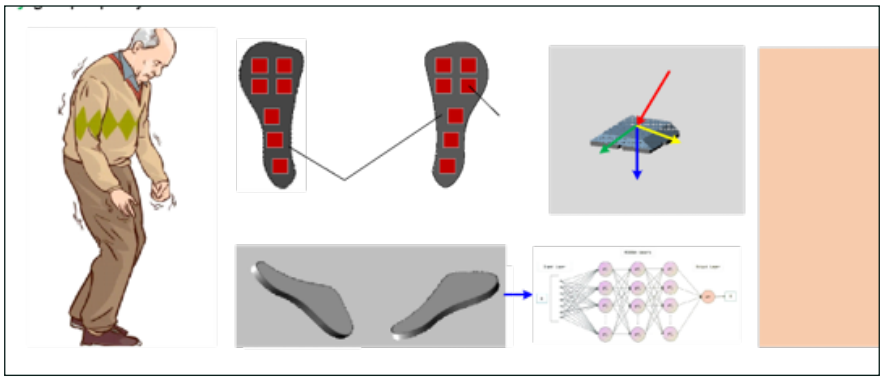


Figure 1: Principle of the 3D plantar force measurement system

Design of 3D Force Sensor

The design of the 3D force-sensing insole centers on a custom mechanical interface that enables the measurement of both normal and shear plantar pressures. A set of shaped silicone pyramids was strategically designed and fabricated using a multi-mold process to serve as force-transducing elements. Each pyramid is coupled with four underlying piezoresistive sensors arranged in a quadrature configuration. When force is applied, the pyramid's geometry deforms differentially—compressing symmetrically under vertical load and tilting asymmetrically under shear—thereby distributing distinct strain patterns to the four sensors. This mechanical arrangement, combined with a calibrated decoupling algorithm, allows the inherently single-axis sensors to resolve the full three-dimensional force vector, transforming a standard pressure insole into a comprehensive sensor for capturing critical gait dynamics.

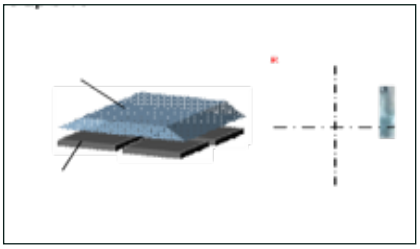


Figure 2: Structure of the 3D Force Sensor

Fabrication of Plantar 3D Force Sensor

The fabrication of the plantar 3D force sensor utilized a layered molding and assembly process to integrate a commercial sensor array with a custom mechanical interface. A full-foot silicone base layer was first cast in a primary mold and adhered directly to the piezoresistive insole, providing a foundational seal. The additional silicone pyramids, each cast in three-dimensional designed molds using a degassed, two-part silicone gel mixture, were then strategically bonded onto this base layer at key plantar pressure points. This modular construction, comprising a uniform substrate and localized anisotropic structures, resulted in a durable, wearable hybrid insole where the off-the-shelf sensors are protected and mechanically coupled to the foot through the custom-designed pyramidal interface, enabling reliable transduction of three-dimensional forces.

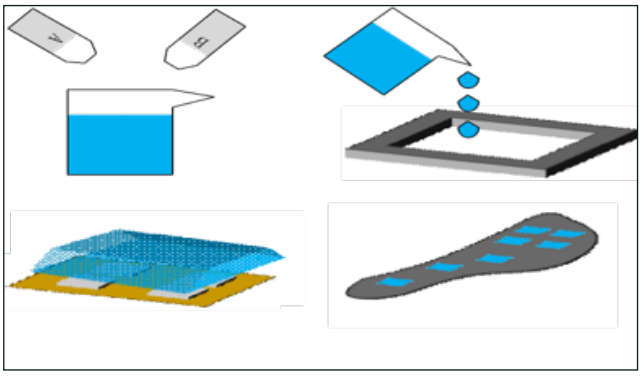


Figure 3: Fabrication Procedure the Fabrication Procedure is Given as:

1. A three-dimensional printed primary mold matching the purchased insole's dimensions was used to shape a thin, uniform base layer. This layer was first adhered to the sensor-insole, providing a foundational platform and comfort.
2. Five secondary molds were designed to fabricate the key pyramidal transducer elements. These pyramids were strategically positioned to correspond with major plantar pressure zones. Their specific geometry was optimized to produce a measurable sensor response that indicated the precise location of each force.
3. Fabrication included a two-part silicone gel. Components A and B were weighed in a 1:1 ratio, mixed thoroughly for two minutes, and degassed in a vacuum chamber to eliminate bubbles that would create mechanical inhomogeneity. Molds were applied with vaseline before pouring the mixture into the molds. After drying, the silicone components were demolded.
4. VI. The final assembly involved bonding the full-foot base layer onto the commercial insole, followed by the precise adhesion of the functional silicone pyramids atop the base layer, directly over their corresponding sensor clusters. This hybrid construction results in a durable, wearable insole that is capable of measuring the true 3D force distribution across the plantar surface.

Force Decouple Model

3D Force Decouple Model

The electrical signals from the four sensors are converted into force components using a calibrated decoupling algorithm. Each sensor's resistance change is first converted to an individual force value using an empirical calibration curve. These four force values are then processed through derived equations to resolve the orthogonal force components (Fy, Fx, Fz). Decoupling coefficients, determined by applying known directional loads with a precision force meter, enable this calculation.

Define a vector force F, and the components of force F along the x, y, z axes are F_x, F_y and F_z, and we have,

$$\mathbf{F} = \sqrt{F_x^2 + F_y^2 + F_z^2} \qquad (1)$$

The decoupling equation can be expressed as,

$$k_x \cdot F_x = \frac{\Delta R_2 / R_2 - \Delta R_4 / R_4}{2} \qquad (2)$$

$$k_y \cdot F_y = \frac{\Delta R_1 / R_1 - \Delta R_3 / R_3}{2} \qquad (3)$$

$$k_z \cdot F_z = \frac{\Delta R_1 / R_1 + \Delta R_2 / R_2 + \Delta R_3 / R_3 + \Delta R_4 / R_4}{4} \qquad (4)$$

where, k_x, k_y and k_z are the decoupling coefficients of **F**; ΔR_1, ΔR_2, ΔR_3 and ΔR_4 are the changing value of the pressure sensor.

We use Eqs.(5)~(6) to calculate k_x, k_y and k_z

$$k_x = \frac{\Delta R_2 / R_2 - \Delta R_4 / R_4}{2} / F_x \quad (5)$$

$$k_y = \frac{\Delta R_1 / R_1 - \Delta R_3 / R_3}{2} / F_y \quad (6)$$

$$k_z = \frac{\Delta R_1 / R_1 + \Delta R_2 / R_2 + \Delta R_3 / R_3 + \Delta R_4 / R_4}{4} / F_z \quad (7)$$

Parameters Calibration

The decouple coefficients k_x, k_y, k_z can be determined by using Eqs.(5), (6), (7). The calculated data are given in Table 1.

Table 1: Decouple Coefficients

Parameters	k_x	k_y	k_z
Value	1.35	1.35	-0.19

Experiment

To validate the proposed 3D piezoresistive measurement system and its integration with the CRNN diagnostic model, a structured experiment was conducted to collect plantar pressure data from both Parkinson's disease patients. The custom in-shoe 3D piezoresistive sensor arrays were connected to a wireless data acquisition module, which transfers voltage readings in real time to a central computer. A custom Python program processed these signals into calibrated three-dimensional force vectors and structured the data from both feet into discrete steps tagged with participant number and timestamp. The program then automatically logged this spatio-temporal data into a designated Google Sheets, enabling persistent, cloud-based storage and immediate remote access for analysis, thereby creating a structured time-series database for AI model training.

By applying this decoupling algorithm to an array of these pyramidal sensing units, the system generates a complete spatio-temporal map of the 3D force distribution across the plantar surface. This rich dataset, encapsulating both magnitude and directional shear forces critical for assessing gait dynamics, forms the direct input for the subsequent Convolutional Recurrent Neural Network (CRNN) analysis for Parkinson's disease diagnosis.

Participant recruitment involved 5 individuals divided into All participants provided informed consent under an approved IRB protocol. The walking protocol was performed on a flat 10-meter walkway. Participants first stood quietly for 30 seconds to record baseline pressure, then performed 20 consecutive trials of walking 10 steps forward at a self-selected pace, turning 180 degrees, and immediately walking 10 steps back to the start. Breaks were offered every five trials to minimize fatigue, yielding approximately 400 steps per participant and capturing gait initiation, continuous walking, and turning dynamics.

The raw time-series data from Google Sheets was then preprocessed prior to the CRNN model input. Using heel-strike events detected from the vertical pressure signal, the continuous data stream was segmented into individual gait cycles. The gait cycle was formatted into a multi-channel 2D matrix (Sensors × Time Steps) for each pressure dimension. This pipeline



Figure 4: Tests of Parkinson's Disease Patients.

The basic information of the participles are given in Table 1.

Table 2: Information of the Participates

Patient no.	Gender	Age	Condition*
1	Male	81	Stage 4
2	Male	82	Stage 3
3	Male	70	Stage 2
4	Male	65	Stage 5
5	Male	80	Stage 3
6	Male	71	Normal
7	Male	51	Normal
8	Female	75	Normal
9	Female	40	Normal
10	Female	24	Normal

Note: The patient's condition is assessed according to the Hoehn and Yahr (HY) Scale.

CRNN Algorithm

As shown in Figure 4, we designed a specialized deep learning architecture named Anti-Overfitting CRNN. The model processes the 3D gait data through three distinct functional modules: a Spatial Encoder (Part 1), a Temporal Encoder (Part 2), and a Classifier Head (Part 3). The data flow and specific layer configurations are detailed below.

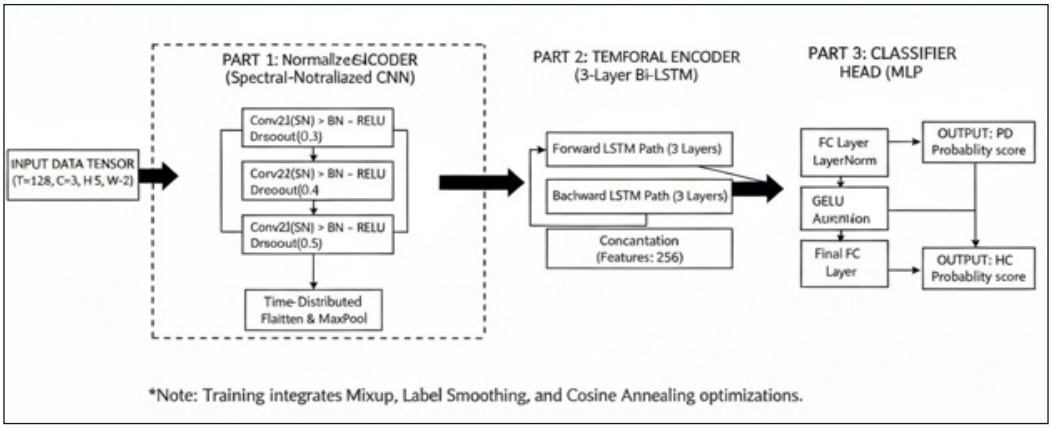


Figure 4: Anti-Overfitting CRNN Architecture

Input Data Representation

The input to the network is a four-dimensional tensor representing the spatio-temporal dynamics of a single gait cycle. Let $X \in R^{T\times C\times H\times W}$ denote the input sample, where $T = 128$ represents the normalized time steps. $C = 3$ corresponds to the three orthogonal force channels Fx, Fy, Fz, capturing the complete 3D force vector at each point.

Crucially, the spatial dimensions $H = 5$ and $W = 2$ represent the topological layout of the sensor array across the plantar surface. These 5×2sensing units are not isolated data points but are spatially arranged to map key anatomical regions, including the heel, midfoot, and forefoot areas. This spatial structure necessitates the use of Convolutional Neural Networks (CNN). By convolving over this grid, the CNN can effectively extract local spatial features, such as the pressure gradient between the medial and lateral sides or the specific force distribution patterns across the metatarsal heads. These spatial correlations are vital for identifying postural instability in Parkinson's disease, which would be lost if the data were simply flattened into a 1D vector.

Part 1: Spatial Encoder (Spectral-Normalized CNN)

The first module, enclosed in the dashed frame in Figure 4, serves as the feature extractor. To mitigate overfitting on our limited dataset, we employed a Spectral-Normalized CNN structure.

Stacked Convolutional Blocks: The input passes through three vertically stacked convolutional blocks. As depicted in the figure, each block consists of a Conv2d layer with Spectral Normalization (SN), followed by Batch Normalization (BN) and ReLU activation.

Progressive Dropout: A key design feature shown in the block diagram is the progressive dropout strategy. The dropout rate increases layer-by-layer from 0.3 in the top block, to 0.4 in the middle, and finally 0.5 in the bottom block. This increasing regularization strength prevents the co-adaptation of deep features.

Dimensionality Reduction: The output of the convolutional stack feeds into the "Time-Distributed Flatten & MaxPool" block, which compresses the spatial dimensions into a compact feature vector for each time step.

Part 2: Temporal Encoder (3-Layer Bi-LSTM)

Following the spatial extraction, the data flows into the Temporal Encoder. As shown in the center of Figure 4, this module utilizes a 3-Layer Bidirectional LSTM (Bi-LSTM) to capture gait dynamics.

Bidirectional Pathways: The architecture splits the processing into two parallel paths: a Forward LSTM Path and a Backward LSTM Path. This structure allows the network to analyze the gait cycle in both chronological (heel-strike to toe-off) and reverse orders.

Feature Fusion: The outputs from both directions converge at the "Concatenation" block, resulting in a fused hidden state with 256 features, which encapsulates the complete temporal context of the walking pattern.

Part 3: Classifier Head (MLP)

The final stage is the Classifier Head based on a Multi-Layer Perceptron (MLP).

Layer Configuration: The fused features first pass through a Fully Connected (FC) Layer followed by LayerNorm. Unlike standard ReLU, we utilized GELU Activation (Gaussian Error Linear Unit) as specified in the architecture, which provides smoother gradient propagation.

Probabilistic Output: The final processing step splits into two terminal nodes, outputting the specific PD Probability score (Parkinson's Disease) and HC Probability score (Healthy Control).

Advanced Optimization Strategy

To further mitigate overfitting and ensure convergence stability, we implemented a multi-faceted optimization strategy:

Mixup Regularization: We employed Mixup training, where virtual training examples are ~ constructed by convex combinations of pairs of inputs and their labels:

$$\tilde{x} = \lambda x_i + (1-\lambda)x_j$$

and

$$\tilde{y} = \lambda y_i + (1-\lambda)y_j$$

examples, reducing the memorization of corrupt labels and increasing robustness to adversarial perturbations.

Label Smoothing: Instead of using hard "one-hot" targets, we utilized “Label Smoothing Cross Entropy” with a smoothing factor ofϵ = 0. 1. This prevents the network from becoming over-confident in its predictions and improves generalization on unseen data.

Cosine Annealing with Warm Restarts: The learning rate is dynamically adjusted using a Cosine Annealing schedule. This periodic decay and restart mechanism allows the model to effectively escape local minima and find flatter, more generalizable basins of attraction in the loss landscape.

Human Test and Analysis

To comprehensively evaluate the performance of our proposed Anti-Overfitting CRNN, we present the quantitative results of the 5-Fold Cross-Validation in Figure 5. This figure aggregates eight sub-plots that visualize the model's accuracy, convergence behavior, and stability from multiple dimensions.

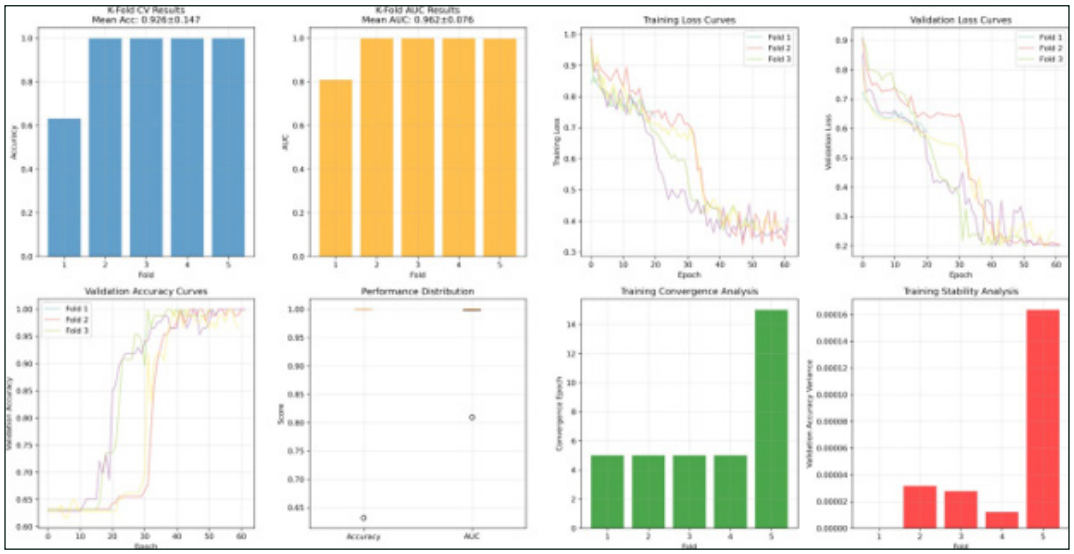


Figure 5: Comprehensive Performance Analysis of the Anti-Overfitting CRNN

Overview of Training Dynamics (Right Panels)

The learning process and model stability are visualized in the right-hand section of Figure 5.

Loss Curves (Top Right): The Training Loss Curves and Validation Loss Curves depict the optimization trajectory over 60 epochs. As shown by the descent of the colored lines, both training and validation losses drop synchronously and stabilize around the 40th epoch. Crucially, the validation loss closely follows the training loss without significant divergence, visually confirming that our regularization strategies (Spectral Norm & Mixup) effectively prevented overfitting.

Convergence Speed (Bottom Right, Green Bars): The Training Convergence Analysis bar chart quantifies how quickly the model learned. We observe that Folds 1-4 converged rapidly (within 5 epochs), whereas Fold 5 (the tall green bar) required significantly more iterations, suggesting that the data in Fold 5 contained more complex or subtle gait features.

Stability Metrics (Bottom Right, Red Bars): The Training Stability Analysis illustrates the variance of the validation accuracy in the final epochs. The relatively low variance for Folds 1-4 indicates that the model settled into a stable solution, while Fold 5 showed higher fluctuations, correlating with its slower convergence.

Classification Performance Evaluation (Left & Center Panels)

The diagnostic capabilities of the system are detailed in the left and center sections of Figure 5.

Accuracy & AUC (Top Left): The K-Fold CV Results (Blue Bars) and K-Fold AUC Results (Orange Bars) present the core performance metrics. The model achieved an impressive Mean Accuracy of 0. 926±0. 147 and Mean AUC of 0. 962±0. 076. Visually, the bars for Folds 2, 3, 4, and 5 reach the 1.0 ceiling, indicating perfect classification on these test sets.

Learning Trajectory (Bottom Left): The Validation Accuracy Curves show the step-wise improvement of diagnostic accuracy. Most folds reached >90% accuracy rapidly between epochs 20 and 30, demonstrating the model's efficiency in extracting 3D gait features.

Statistical Distribution (Bottom Center): The Performance Distribution boxplot summarizes the spread of the results. The tight grouping of the box and whiskers at the top (1.0) for both Accuracy and AUC confirms the robust reproducibility of our method across most subjects.

Error Analysis: The Fold 1 Outlier

Despite the overall high performance, Figure 5 reveals a notable anomaly.

Visual Observation: In the K-Fold CV Results (Blue Bars), the bar for Fold 1 is significantly lower (~0.63) compared to the others. Similarly, the Performance Distribution boxplot shows a distinct outlier point below the main cluster.

Clinical Interpretation: Since this study employs a Leave-One-Subject-Out validation scheme, "Fold 1" corresponds to a specific test participant. This performance drop suggests that this particular patient exhibited atypical or early-stage gait symptoms (e.g., less pronounced shear force deviations) that were statistically closer to the healthy control group.

Implication: This outlier highlights the inherent heterogeneity of Parkinson's disease. While our model perfectly diagnosed 80% of the cases (4 out of 5 subjects), the Fold 1 result emphasizes the necessity of expanding the dataset in future work to capture a wider spectrum of symptom severity and improve the model's sensitivity to atypical cases.

Conclusion

In this work, we presented a 3D planar force measurement system for the estimation of Parkinson's patients. We designed the 3D force sensor and the wearable in-shoe device. And test its performance on Parkinson's disease diagnosis. The main contributions of our work are:

- Designed three-dimensional force measurement technology
- Calculate tangential plantar pressure data using decoupling algorithms
- Obtain data from Parkinson's patients and normal people
- Used a CRNN model to find symptoms of Parkinson's
- Utilizing the differences in three-dimensional plantar pressure between healthy individuals and Parkinson's disease patients for the diagnosis and assessment of Parkinson's disease

Building on the 3D plantar pressure measurement system and CRNN-based diagnostic framework established in this work, several promising directions for future research and development are envisioned. The immediate next step involves the development of a dedicated mobile application to enhance accessibility, usability, and clinical utility. This app would serve as a user-friendly interface for patients and clinicians, allowing for the seamless upload of sensor data collected during prescribed walking protocols directly to a secure cloud server. The uploaded spatio-temporal pressure data would be automatically formatted and fed into a trained AI model, generating a preliminary diagnostic assessment or progression report that is relayed back to the user and their healthcare provider. This integrated ecosystem would enable remote monitoring, facilitate long-term tracking of symptom progression, and provide a tool for evaluating treatment efficacy outside clinical settings.

Furthermore, the rich dataset of three-dimensional plantar pressure contains information that extends beyond Parkinson's disease. Future work will investigate the system's capability to detect and characterize other neurological and musculoskeletal conditions that manifest in gait and pressure distribution anomalies. This includes, but is not limited to, other neurodegenerative disorders (e.g., Huntington's disease, multiple system atrophy), stroke-related gait impairments, diabetic peripheral neuropathy, and conditions affecting balance and posture. Expanding the AI model into a multi-task or multi-class classification framework would require the collection of new, labeled datasets for these additional conditions. The ultimate goal is to evolve the platform into a comprehensive digital biomarker tool for movement disorders, capable of providing differential diagnostic support and continuous, quantitative mobility assessment. Continued refinement of the sensor hardware for comfort and durability, alongside validation through large-scale longitudinal clinical studies, will be critical to translating this research into a practical tool for early detection and personalized management of a spectrum of movement-related diseases.

Reference

1. Sidransky E, Nalls MA, Aasly JO (2009) Multicenter analysis of glucocerebrosidase mutations in Parkinson's disease. New England Journal of Medicine 361: 1651-1661.
2. Dong S, Cui Y (2025) Projections for prevalence of Parkinson's disease and its driving factors in 195 countries and territories to 2050: modelling study of Global Burden of Disease Study 2021. BMJ 388.
3. Herbers C, Zhang R, Erdman A (2024) Distinguishing

features of Parkinson's disease fallers based on wireless insole plantar pressure monitoring. npj Parkinson's Disease 10: 67.

4. Hadi A, Razak A, Zayegh A, Begg RK, Wahab Y (2012) Foot plantar pressure measurement system: a review. Sensors 12: 9884-9912.
5. Dong L (2024) Rational design of flexible mechanical force sensors for healthcare and diagnosis. Sensors and Actuators A: Physical 12: 105.
6. Islam MA, Majumder MZH, Hussein MA, Hossain KM, Miah MS (2024) A review of machine learning and deep learning for Parkinson's disease detection using handwriting and voice datasets. Heliyon e25469.

Copyright: ©2026 Terry Zhang. This is an open-access article distributed under the terms of the Creative Commons Attribution License, which permits unrestricted use, distribution, and reproduction in any medium, provided the original author and source are credited.